

Thermal emission of midinfrared GaAs photonic crystals

Estelle Homeyer, Julien Houel, Xavier Checoury, Guy Fishman, Sébastien Sauvage, and Philippe Boucaud*

Institut d'Electronique Fondamentale, CNRS-Université Paris Sud, Bâtiment 220, 91405 Orsay, France

Stéphane Guilet, Rémy Braive, Audrey Miard, Aristide Lemaître, and Isabelle Sagnes

Laboratoire de Photonique et de Nanostructures, CNRS, Route de Nozay, 91406 Marcoussis, France

(Received 23 July 2008; revised manuscript received 11 September 2008; published 6 October 2008)

We have investigated the thermal emission of midinfrared dielectric photonic crystals. We show that the optical properties of the photonic crystals can be probed by the photomodulation of the room-temperature thermal emission. The technique is illustrated in the case of membrane-type two-dimensional photonic crystals. The GaAs-based photonic crystal membranes were fabricated by wafer bonding followed by standard e-beam lithography and etching processes. Thermal radiation collected from the surface of the sample allows one to investigate experimentally a broad spectral range from 500 to 1500 cm^{-1} . Zone-center modes at the Γ point coupled to the radiative continuum are evidenced around 900 cm^{-1} (11 μm wavelength). The lattice periodicity of the photonic crystals allows one to spectrally tailor the emissivity. Three-dimensional finite-difference time-domain modeling is used to explain the thermal radiation spectra of the photonic crystal characterized by optical sources embedded in the whole structure.

DOI: [10.1103/PhysRevB.78.165305](https://doi.org/10.1103/PhysRevB.78.165305)

PACS number(s): 42.70.Qs, 78.30.-j, 65.90.+i

I. INTRODUCTION

Photonic crystals are artificial structures with a periodical modulation of material permittivity. The emissivity of photonic crystals has attracted considerable interest over the last years following the early claims of enhanced thermal emissivity in these structures as compared to blackbody emission in free space.¹ It was later demonstrated either by thermodynamic arguments² or by a direct calculation of thermal radiation³ that the optical properties of the photonic crystals could be derived from equilibrium thermodynamic laws and that a photonic crystal does not emit more than a blackbody. The ability of photonic crystals to spectrally and directionally tailor the thermal emission remains, however, of great importance. From Kirchoff's law, an object in thermal equilibrium with its surrounding radiation field has equal absorptivity and emissivity for a given frequency, polarization, and direction. The directional emissivity of a thin slab at a given frequency is given by the ratio of the optical power per unit area emitted in a solid angle and the optical power per unit area emitted by a blackbody at the same temperature. The emissivity of a film for a solid angle $d\Omega_{\mathbf{k}}$ is thus given by $\xi_{\mathbf{k}}(\omega) = A_{\mathbf{k}}(\omega) = 1 - R_{\mathbf{k}}(\omega) - T_{\mathbf{k}}(\omega)$ where A , R , and T are the absorptivity, reflectance, and transmittance of the film.⁴ The power spectrum of the film is then given by the product of the emissivity times the same temperature Planck blackbody power spectrum. The sample can thus be fully characterized by the reflectivity and transmission. However, the simultaneous measurement at different wave vectors of reflectivity and transmission can be in some cases very difficult to obtain and even impossible in the case of semitransparent membranes on absorbing substrates. Experimentally, the spectral emissivity measurement is thus challenging. The knowledge of the optical properties of photonic crystals is, however, a prerequisite in order to tune their properties and use them in photonic devices. In the midinfrared spectral range, two-dimensional photonic crystals were introduced in order to obtain normal-incidence emission in quantum cascade lasers⁵

or in order to reduce the threshold of quantum cascade lasers.⁶ Photonic crystals could also be used to enhance the spontaneous emission rate and the collection efficiency of quantum dot intersublevel emission, and provide cavities to demonstrate a quantum dot intersublevel polaron laser.⁷

The usual methods to characterize photonic crystals are either to couple light from an external source or to embed an internal source inside the photonic crystal. The internal source approach has been successfully implemented to characterize GaAs (Ref. 8) or silicon-based photonic crystals.^{9,10} For photonic crystals operating in the midinfrared spectral range, a standard approach to analyze their properties is to measure the thermal radiation by performing measurements at elevated temperatures in order to get rid of the background emissivity.¹¹ This approach can be limited in some cases since it can be difficult to selectively heat a photonic crystal with reduced dimensions at high temperature and without damage. Another approach to investigate the optical properties is to use the room-temperature emissivity of the photonic crystal. The room-temperature thermal radiation offers several advantages: it is intrinsically available; it covers a very broad spectral range much larger than the spectral range covered, for example, by semiconductor quantum dot emission (ca. 10% around the resonance energy); and the thermal emissivity is very convenient to measure light coupled perpendicular from the surface or close to normal incidence.

In this work, we introduce a technique to characterize midinfrared photonic crystals based on a photomodulation of the photonic crystal thermal radiation. The photomodulated change of emissivity is spectrally investigated over a broad spectral range. The measurement differs from standard photothermal or photocarrier radiometry measurements.^{12,13} In the latter cases, the modulated infrared signal is spectrally integrated over the detector bandwidth and the modulated signal reflects the sample absorption and carrier and thermal diffusion dynamics. The photomodulation of thermal radiation is illustrated for the case of GaAs photonic crystal membranes exhibiting resonant modes in the midinfrared spectral

range. A large number of studies have been devoted to photonic crystal membranes in a planar geometry in the near infrared.¹⁴ Since the midinfrared photonic crystals are significantly different by their dimensions from standard near-infrared photonic crystal membranes, we have developed a method to fabricate photonic crystal membranes both for the midinfrared spectral range and in a planar geometry. The planar geometry was chosen for its facility for processing. We show that the photomodulation can probe zone-center modes of the photonic crystals. It provides useful information on the mode resonances and is well suited to investigate the out-of-plane emission emitted perpendicular to the surface of two-dimensional photonic crystals. The thermal emission is also significantly different from the standard characterization of photonic crystals with an internal source. In the latter case, a single-quantum dot layer is usually inserted in the middle of a membrane. For thermal emission measurements, all the volume of the membrane contributes to the signal and the radiated patterns differ significantly from those obtained in the single-quantum dot layer case.

II. GaAs MIDINFRARED PHOTONIC CRYSTAL

A specific technology was developed to realize photonic crystal suspended membranes on GaAs substrates since the standard fabrication techniques for near-infrared photonic crystals cannot be directly transposed to the midinfrared. The sample was grown by molecular-beam epitaxy. An AlGaAs stop-etch layer containing 80% of aluminum was first deposited on the GaAs substrate. A 3 μm thick GaAs layer was then epitaxially grown on it. Layers of InAs self-assembled quantum dots were embedded in the structure. The quantum dots do not play any significant role in the following experiments. The sample was covered by a 7 μm thick oxide layer deposited by plasma-enhanced chemical vapor deposition. This was followed by the deposition of Ti/Au and In/Au metallic layers. Thanks to these metallic layers, the sample was then bonded on a second handle GaAs substrate. The substrate of the first wafer was removed by wet chemical etching down to the AlGaAs stop-etch layer. The photonic crystals were then patterned by e-beam lithography following a triangular lattice. The lattice periodicity was varied between 5.5 and 6.5 μm . Circular air columns were then etched down to the oxide layer by inductively coupled plasma etching. In the final step, the oxide layer was removed by wet etching in fluorydric acid, leaving a suspended GaAs membrane. Figure 1 shows images of the fabricated photonic crystals. Figure 1(a) shows a top view scanning electron micrograph image of the photonic crystal. Figure 1(b) shows a cross section of the GaAs suspended membrane which is separated from the substrate by a 7 μm thick air gap. The AuIn₂ metallic bonding can be observed at the interface between the substrate and the air gap. The advantage of the process is to provide membranes with a good mechanical stability on a thick GaAs substrate. The 3 μm thickness of the GaAs layer corresponds to a $\frac{\lambda}{2n}$ thickness for a 20 μm wavelength. The air hole radius is around 0.35 a where a is the lattice periodicity. The number of periods are around ten in order to take advantage of the photonic crystal

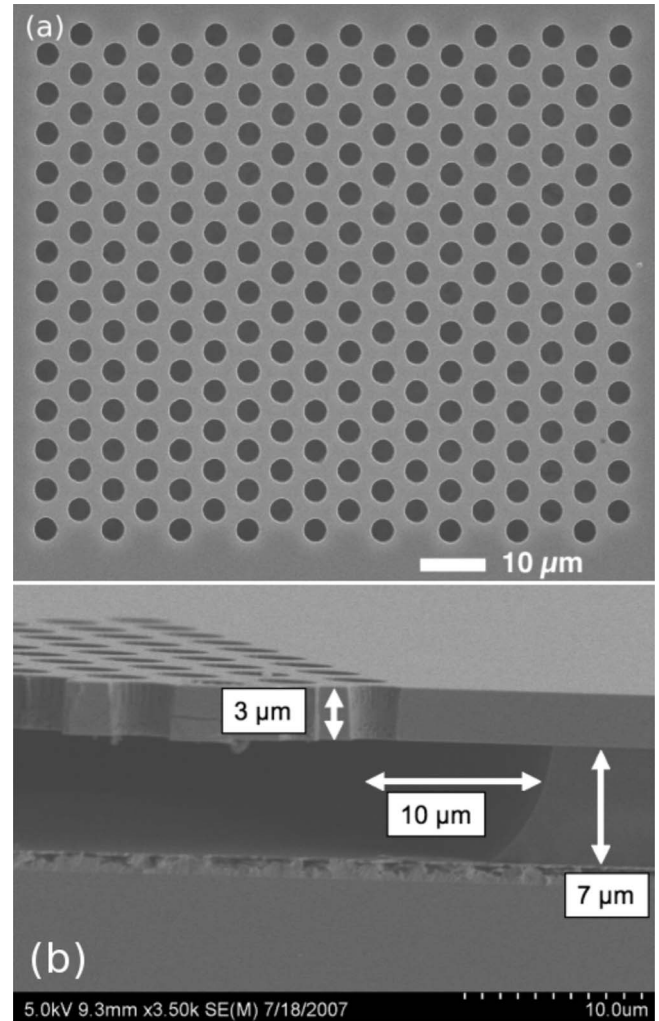


FIG. 1. (a) Top view scanning electron micrograph image of the planar two-dimensional photonic crystal membrane. (b) Cross section of the photonic crystal membrane. The bonding metallic layer is observed at the interface between the air gap and the GaAs substrate.

effect while keeping a good mechanical stability for the membrane.

III. EXPERIMENTAL SETUP

For emissivity measurements, the photonic crystal sample is placed on the emission port of a Fourier transform infrared spectrometer. The photomodulated thermal emission measurement is performed at room temperature. The photonic crystal is illuminated by an argon-ion laser focused on the whole photonic crystal surface (i.e., $\approx 100 \times 100 \mu\text{m}^2$). The incident visible light is modulated by a mechanical chopper at low frequency (200 Hz). The incident power is around 100 mW. The emission is collected by gold-coated parabolic mirrors with a numerical aperture of 0.2 and detected by a nitrogen-cooled mercury cadmium telluride photodetector. The spectrometer is operated in step-scan mode. The modulated signal is filtered by a lock-in amplifier before being injected into the acquisition board of the spectrometer. The

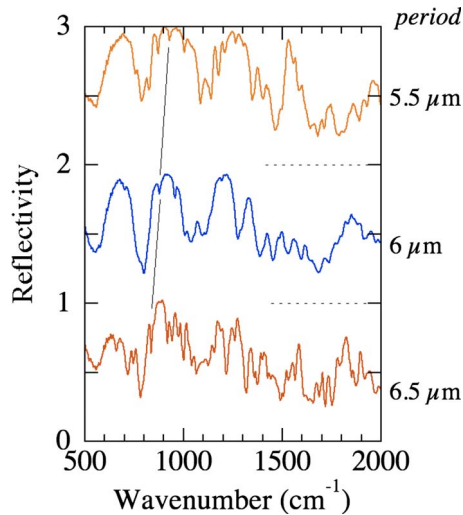


FIG. 2. (Color online) Reflectivity spectra of photonic crystals with different lattice periodicities (6.5, 6, and 5.5 μm from bottom to top). The curves have been offset for clarity; dashed lines show the reference zero for the offset curves. A resonant peak corresponding to a zone-center mode at the Γ point which is also observed in emissivity measurements is outlined.

carriers generated by the absorption of the visible excitation in the GaAs membrane change the free-carrier absorption of the material and its temperature. It therefore modifies the emissivity which is synchronously recorded at the chopping frequency. The measurement is differential and therefore background free. The amplitude of the signal exhibits a linear dependence as a function of the input power. The reflectivity of the samples was measured with a microscope coupled to the infrared spectrometer. The microscope is equipped with $\times 15$ Cassegrain mirrors. The reflectivity is integrated for incidences varying between 15° and 45° . A mask placed at a focal plane allows us to spatially select the sole reflectivity of the photonic crystal structure.

IV. RESULTS

Figure 2 shows the reflectivity spectra of the photonic crystal membranes with different lattice parameters (6.5, 6, and 5.5 μm). The reflectivity drops above 1500 cm^{-1} . For normal incidence, the incident light has no k transverse component. Because of the periodicity, it can only couple to modes with wave vectors which are an integer multiple of $\frac{2\pi}{a}$ where a is the lattice parameter. Additional nonorthogonal diffraction directions which allow out-of-plane coupling at angles different from 90° start to appear above the normalized frequency $u = \frac{a}{\lambda} = 1$ which corresponds to 1540 cm^{-1} for a lattice periodicity of 6.5 μm . The energy of reflectivity roll-off increases as the lattice periodicity is reduced. The reflectivity is dominated by Fabry-Pérot oscillations. The Fabry-Pérot oscillations correspond to the reflectivity associated with the 3 μm thick membrane with reflectivity minima around 550 and 1100 cm^{-1} . Additional periods appear because of the 7 μm thick air gap and the metallic layer beneath which increases the length for the Fabry-Pérot oscilla-

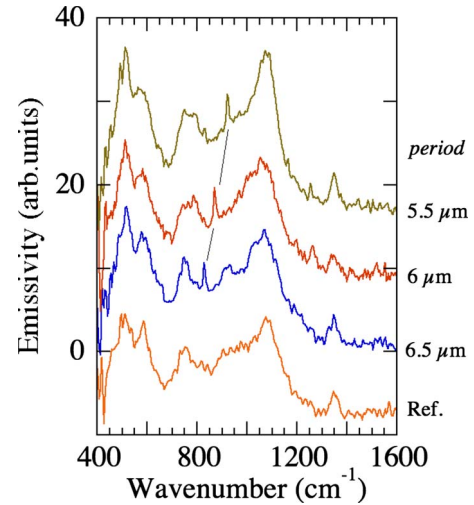


FIG. 3. (Color online) Room-temperature photomodulated thermal emission of three photonic crystal structures with different lattice periodicities. A reference spectrum of the GaAs layer on oxide measured outside of the photonic crystal patterns is also shown. The curves have been offset for clarity. Apart from the Fabry-Pérot resonances of the GaAs membrane, a resonant band-edge mode is observed between 830 and 940 cm^{-1} and shifts to high energy as the lattice periodicity is reduced.

tions. These additional periods are observed around 780 and 1560 cm^{-1} . A large number of narrow resonances with linewidths around 10 cm^{-1} are superimposed on the Fabry-Pérot oscillations. They correspond to reflectivity changes larger than 10%. The noise level which is below 2% is hardly observed in the figure. These resonances are the signature of photonic crystal optical modes. For the sample with the 6.5 μm lattice periodicity, the first resonance is observed around 660 cm^{-1} , which corresponds to a normalized frequency of 0.43. The onset of photonic crystal reflectivity peaks around the normalized frequency of 0.43 is in agreement with the calculated reflectivity spectrum of the photonic crystal. Additional peaks are observed at 840 cm^{-1} and above. The amplitude of the reflectivity minima is not constant when the lattice periodicity is modified. The spectral shift as a function of the lattice periodicity can, however, be followed. As highlighted on the figure, the reflectivity dip at 840 cm^{-1} for the 6.5 μm sample shifts to 880 and 930 cm^{-1} when the lattice periodicity is decreased. As will be shown below, this resonance is the one which is more clearly evidenced by photomodulated thermal emission measurements.

Figure 3 shows the photomodulated thermal emission for three different photonic crystal structures as compared to a reference spectrum recorded between the photonic crystal patterns. The spectra have been normalized from the photodetector and beam splitter response. Between the photonic crystal patterns, the GaAs layer lies on the oxide layer. The spectral range covered is quite large going from 400 to 1400 cm^{-1} . The low energy cutoff is given by the photodetector response. In normalized frequency, the spectral range covered by the modulated photothermal emission goes roughly from 0.25 to 1 which is quite significant as compared to standard internal source characterizations which are

usually limited to 10–20% around the maximum. Broad resonances are observed around 550, 770, and 1080 cm^{-1} at positions which correspond to the minima at 550, 780, and 1100 cm^{-1} observed in Fig. 2. These resonances are associated with the Fabry-Pérot resonances of the GaAs membrane. They correspond to a minimum of reflectivity as observed in Fig. 2. For a perfectly absorbing layer, the emissivity would be proportional to $1-R$ where R is the reflectivity of the interface, the emissivity peaks are thus correlated with the reflectivity minima. The resonance around 550 cm^{-1} is reinforced by the GaAs two-phonon absorption at 520 cm^{-1} .¹⁵ The comparison between the reference spectrum and the spectra measured with the photonic crystal membranes shows that the bulk layer on oxide provides a significant contribution to the photomodulated thermal emission as a result of thermal diffusion. This feature is a consequence of the detector size (1 mm^2) which integrates a signal outside of the photonic crystal pattern. Superimposed on the Fabry-Pérot oscillations, one can observe a resonant peak around 830 cm^{-1} for the 6.5 μm sample which shifts to high energy as the lattice parameter is decreased. This resonant peak corresponds to a zone-center mode of the photonic crystal with a normalized frequency of 0.54. Its normalized frequency remains nearly constant as the lattice periodicity is modified decreasing to 0.52 and 0.51 for the 6 and 5.5 μm samples. The small variation of normalized frequency is attributed to a change of the air filling factor of the photonic crystal as observed by scanning electron micrographs. The normalized frequency of the zone-center mode is in agreement with the value calculated for the membrane structure by a two-dimensional plane-wave method, as will be explained below. In the photonic crystal, waves propagating in different directions can couple because of the lattice periodicity. Coupled light can be emitted perpendicular to the surface following first order Bragg diffraction.¹⁶ This mechanism which appears for zone-center modes at the Γ point is identical to the one used for grating coupled surface emitting lasers. In the present case, Bragg diffraction couples light propagating in different in-plane directions. The observation of such a zone-center mode indicates that the photomodulated thermal emission is appropriate to investigate the optical properties of two-dimensional photonic crystals. The mode at the normalized frequency of 0.54 is also observed on the reflection spectra. However, all the narrow resonances observed on the reflectivity spectra are not observed on the photomodulated emission spectra. First, we note that both measurements are not performed with the same optical incidences and the same numerical apertures. It can obviously introduce some discrepancies between both measurements through peak broadening and k vector dependence of the radiated patterns. Moreover, only the modes with strong field overlap with the GaAs material can be observed in photomodulation measurements. The optical modes with a large field localization in the air hole modes cannot be observed in the emissivity measurements. The direct observation of the emissivity is thus mandatory in order to correctly identify the optical modes which can effectively be coupled perpendicular from the surface of the sample.

In transverse electric (TE) polarization and for an effective index of 3 at 10 μm , the photonic diagram of the trian-

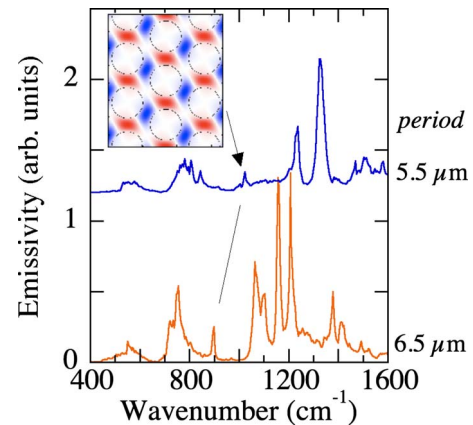


FIG. 4. (Color online) Room-temperature emissivity spectra of photonic crystal membranes calculated by a three-dimensional finite-difference time-domain scheme. The optical sources are distributed within the whole photonic crystal membrane. The collection numerical aperture is 0.2. The curves are shown for two different lattice periodicities (6.5 and 5.5 μm). The resonance corresponding to the experimentally observed Bloch mode at the Γ point is highlighted. The H_z profile of the mode is shown in the inset.

gular lattice pattern obtained by a two-dimensional plane-wave calculation exhibits a zone-center mode at the Γ point at a normalized frequency of 0.46 and three zone-center modes at a normalized frequency around 0.55, including two degenerate quadrupole modes and a monopole mode. The group-velocity dispersion is different for the three Bloch modes, and the quadrupole mode with the lower group velocity provides a better lateral photon confinement and is thus likely to dominate the radiation pattern. This can be confirmed by the emissivity modeling. For this purpose, we have performed finite-difference time-domain (FDTD) calculations of the emissivity. Following Kirchoff's law, the emissivity should be equal to $1-R-T$. Instead of calculating and integrating the reflectance and transmittance over all the incidences, we have calculated the far-field spectra of the photonic crystal membrane with a large density of embedded optical sources inside the membranes. The phases of the optical sources are chosen randomly in order to avoid coherent effects. These sources mimic the broad spectral thermal emission. The sources are turned on during all the simulation time. The spectral power spectrum is then obtained using the periodogram method. The losses introduced by the metallic layer are taken into account through a finite conductivity. The radiated spectrum is then multiplied by a Planck distribution at room temperature. A specific feature of the measurement is that the corresponding internal source is distributed all over the photonic crystal membrane, i.e., not only at the middle of the slab. The emissivity outside of the photonic crystal pattern which results from thermal diffusion in the GaAs layer on oxide is not taken into account in the modeling. The modeling thus reflects the difference between the photonic crystal spectra of Fig. 3 and the reference spectrum shown at the bottom of Fig. 3. Figure 4 shows the calculated radiated spectra of the two-dimensional photonic crystal membrane as integrated with a numerical aperture of 0.2. The calculated radiation spectra are shown for two different

lattice periodicities, 6.5 (bottom) and 5.5 μm (top). For the structure with a 6.5 μm lattice periodicity, a radiated mode is clearly observed at 900 cm^{-1} . It corresponds to the photonic crystal mode which is experimentally evidenced at 830 cm^{-1} . The energy difference between 830 and 900 cm^{-1} can be accounted for by the uncertainty on the refractive index and thickness of the membrane and by a small deviation between the experimental air filling factor and the one used in modeling. This mode shifts as expected to high energy when the lattice periodicity is decreased. Additional resonant modes are observed on the calculated radiation spectra around 750, 1050, and 1200 cm^{-1} . A careful analysis of the emissivity spectra for the 6.5 μm lattice periodicity as compared to the reference spectrum indicates that a mode with a large broadening is present around 925 cm^{-1} in Fig. 3. This mode likely corresponds to the calculated resonance of the dipole mode around 1050 cm^{-1} . At higher energy, the visibility of the different modes is reduced because of the background signal originating from the GaAs layer on oxide. Moreover, additional losses, the sensitivity to roughness which is more important at high energy, and a deviation from a perfect structure can explain that the modes around 1200 cm^{-1} are not experimentally observed. As shown in Fig. 4, the relative amplitude of the different modes is strongly dependent on the lattice periodicity. Moreover, the limited thickness between the membrane and the buried metallic layer which is of the order of the wavelength introduces an additional phase matching condition which depends both on the wavelength and on the exact reflection properties of the AuIn₂ layer. The important feature is that the FDTD calculations confirm that the quadrupole Bloch mode at the

normalized frequency of 0.54 is coupled to the radiative continuum as experimentally observed.

V. CONCLUSION

We have introduced a different technique to characterize two-dimensional photonic crystals which is based on the photomodulation of the room-temperature emissivity. A specific feature of this technique is that the corresponding internal source is distributed all over the photonic crystal membrane and is spectrally broad. This technique was illustrated in the case of GaAs membrane-type photonic crystals processed in a planar geometry. The parameters of the photonic crystals were chosen in order to obtain resonant optical modes in the spectral range of the room-temperature blackbody emission. We have shown that the emissivity spectra differ significantly from the experimental reflectivity spectra. Only a smaller number of modes can be efficiently coupled perpendicular to the surface in emissivity as compared to reflectivity. A zone-center Bloch mode at the Γ point, which corresponds to a quadrupole mode, is clearly evidenced around 900 cm^{-1} , i.e., 11 μm wavelength. The experimental measurements are supported by three-dimensional modeling of the emissivity using a finite-difference time-domain scheme. Our results indicate that the photomodulated thermal emission at room temperature is a very useful technique to investigate midinfrared photonic crystals.

ACKNOWLEDGMENTS

This work was supported by the French National Research Agency ANR-PNANO program QUOCA.

*philippe.boucaud@ief.u-psud.fr. URL: <http://pages.ief.u-psud.fr/QDgroup/index.html>

¹S. Y. Lin, J. Moreno, and J. G. Fleming, *Appl. Phys. Lett.* **83**, 380 (2003).

²T. Trupke, P. Wurfel, and M. A. Green, *Appl. Phys. Lett.* **84**, 1997 (2004).

³C. Luo, A. Narayanaswamy, G. Chen, and J. D. Joannopoulos, *Phys. Rev. Lett.* **93**, 213905 (2004).

⁴C. M. Cornelius and J. P. Dowling, *Phys. Rev. A* **59**, 4736 (1999).

⁵R. Colombelli, K. Srinivasan, M. Troccoli, O. Painter, C. F. Gmachl, D. M. Tennant, A. M. Sergent, D. L. Sivco, A. Y. Cho, and F. Capasso, *Science* **302**, 1374 (2003).

⁶M. Lončar, B. G. Lee, L. Diehl, M. A. Belkin, F. Capasso, M. Giovannini, J. Faist, and E. Gini, *Opt. Express* **15**, 4499 (2007).

⁷S. Sauvage and P. Boucaud, *Appl. Phys. Lett.* **88**, 063106 (2006).

⁸D. Labilloy, H. Benisty, C. Weisbuch, C. J. M. Smith, T. F.

Krauss, R. Houdre, and U. Oesterle, *Phys. Rev. B* **59**, 1649 (1999).

⁹S. David, M. El Kurdi, P. Boucaud, A. Chelnokov, V. Le Thanh, D. Bouchier, and J. M. Lourtioz, *Appl. Phys. Lett.* **83**, 2509 (2003).

¹⁰M. El Kurdi, X. Checoury, S. David, T. P. Ngo, N. Zerounian, P. Boucaud, O. Kermarrec, Y. Campidelli, and D. Bensahel, *Opt. Express* **16**, 8780 (2008).

¹¹C. H. Seager, M. B. Sinclair, and J. G. Fleming, *Appl. Phys. Lett.* **86**, 244105 (2005).

¹²S. O. Kanstad and P-E. Nordal, *Appl. Surf. Sci.* **6**, 372 (1980).

¹³A. Mandelis, J. Batista, and D. Shaughnessy, *Phys. Rev. B* **67**, 205208 (2003).

¹⁴O. Painter, R. K. Lee, A. Scherer, A. Yariv, J. D. O'Brien, P. D. Dapkus, and I. Kim, *Science* **284**, 1819 (1999).

¹⁵J. S. Blakemore, *J. Appl. Phys.* **53**, R123 (1982).

¹⁶M. Imada, A. Chutinan, S. Noda, and M. Mochizuki, *Phys. Rev. B* **65**, 195306 (2002).